X-661-75-232
PREPRINT

NASA TM X- 71017

RESULTS FROM THE ARIEL-5 ALL-SKY X-RAY MONITOR

STEPHEN S. HOLT

SEPTEMBER 1975

GSFC

GODDARD SPACE FLIGHT CENTER
GREENBELT, MARYLAND

RESULTS FROM THE ARIEL-5 ALL-SKY MONITOR

Stephen S. Holt
Laboratory for High Energy Astrophysics
Goddard Space Foight Center
Greenbelt, Maryland 20771 USA

Abstr^ct: A summary of results obtained from the first year of Ariel-5 All-Sky Monitor operation is presented. Transient source observations, as well as the results of long-term studies of Sco X-1, Cyg X-3 and Cyg X-1 are described. By example, the included results are indicative of the temporal effects to which the All-Sky Monitor remains sensitive as it begins its second year of observation.

Invited paper presented to the
Royal Society, London, 14 October 1975

1. INTRODUCTION The All-Sky Monitor is a small, low sensitivity instrument devoted to the full-time study of the entire celestial sphere. Its objectives are the identification of transient x-ray intensity variations in both known and new x-ray sources, as well as the search for regularity in the temporal variations from strong sources which a long continuous observation may allow. It has operated without fault for one year, during which time a variety of x-ray phenomena in these categories have been observed. This paper summarizes some of the work accomplished during this first year of Ariel-5 operation.

2. EXPERIMENT The All-Sky Monitor consists of a pair of x-ray pinhole cameras which have an instantaneous fan beam acceptance angle of 4° FWHM which extends from the spacecraft spin axis to anti-spin axis. This fan beam is carried around by the spacecraft rotation so that the whole sky is swept once each satellite spin period. The important instrument parameters are an effective pinhole area of $0.6cm^2$ in the band 3-6 keV, a duty cycle for source observation of $\sim 1\%$, and a temporal resolution of one orbit (100 minutes) during which time the sky is divided into 512 resolution elements ($\sim 10°x10°$). The 3-6 keV window is almost totally insensitive to source spectral form, assuring a monitor function which is dependent upon intensity alone. Approximately 20% of the sky is not monitored each orbit, as there are instrument dead bands at the spacecraft poles and equatorial plane; the fields-of-view of the other Ariel-5 experiments are, therefore, mutually exclusive of that of the All-Sky Monitor. A detailed description of the experiment operation and sensitivity may be found in Holt (1975). Over an observation time of $\frac{1}{2}$-day, the average sensitivity is $\sim 10\%$ of the intensity of the Crab Nebula.

3. TRANSIENT SOURCE OBSERVATIONS There have been more transient sources observed during the first year of Ariel-5 operation than during the preceding decade. The reason is primarily the excellent coverage which the spacecraft affords, rather than a particularly anomalous year for transient phenomena.

The first detected was the source in Triangulum first reported from the Ariel-5 Sky Survey Experiment (Pounds, 1974). As shown in Figure 1 from Kaluzienski, et al. (1975), the source exhibits some of the characteristics of previously identified transients: a relatively rapid rise (relative to decay), a drop to an apparent plateau during which the decay is very slow, and a final decay with a timescale of $\sim$ 2 months. The spectrum was similarly reminiscent of earlier sources, being softer than that of the Crab Nebula. The new characteristics observed by the combination of the Sky Survey and All-Sky Monitor experiments are a variable extended pre-maximum on-state for the source, during which time the spectrum softens. Such a gradual erratic increase to maximum may preclude an association with thermonuclear models which have been put forth for transient sources (as they typically involve a slow buildup of fuel without x-ray production until they flash), and the spectral softening up to a maximum suggests a source which may be Eddington-limited at its onset.

The next transient, Cen X-mas (Ives, Sanford and Bell Burnell, 1975) was out of the All-Sky Monitor field-of-view at the spacecraft pole for its entire lifetime. Very unlike the Triangulum source, it exhibited a spectrum much harder than the Crab and an e-folding decay time of only one week. It also was the first source discovered to be regularly modulated on a time scale of the order of minutes, and was, at maximum, < 25% of the apparent magnitude of the Crab Nebula in x-rays. Like the situation for Cen X-mas, no substantial data was accumulated for the third Ariel-5 transient (near galactic center) in this case owing to the source confusion in such a congested region of the galaxy. The All-Sky Monitor detected it near maximum at a level in excess of the Crab Nebula, but could not follow its decay. It would appear, however, that its x-ray characteristics were much closer to those of Triangulum than those of Centaurus.

The fourth transient, in Taurus, appeared at the spacecraft pole during an extended stop at the Crab Nebula. Although the All-Sky Monitor missed the onset, (Eyles, et al. 1975), the decay was followed after the spin axis moved off the source (Kaluzienski, Holt, Boldt and Serlemitsos, 1975). In all respects, this source closely resembles Cen X-mas (e.g. hard spectrum, $\sim$ minute pulsing). With an intensity at maximum close to that of the Crab Nebula, the same sort of very regular decay was observed (in this case, with an e-folding time of $\sim$ 19d).

Although not formally a transient, a flare measured from Aql X-1 in June was almost indistinguishable from the operational definition of such an object. Increasing to the level of the Crab Nebula from an intensity two orders-of-magnitude lower during the previous two years, the profile of the rise and decay of Aql X-1 is quite similar in shape to the profile of the Triangulum source, with the temporal scale compressed. It may, therefore, represent an important clue to the nature of "ordinary" transients of the Triangulum variety, in much the same way as the ~ minute modulation and hard spectrum of Vela X-1 is a useful hint at the nature of the Centaurus and Taurus transients.

Finally, the fifth (and most spectacular) source is A0620-00. Discovered during a > one-month extended hold of the spacecraft equatorial plane in coincidence with the galactic plane (Elvis, et al. 1975), the onset was once again out of the All-Sky Monitor field-of-view. As shown in Figure 4, the experiment can see the source briefly shortly after maximum, indicating a peak 3-6 keV intensity at more than 4 times Sco X-1. The decay is quite regular, and apparently slowing down with time. The All-Sky Monitor will be able to follow the decay for another two decades in intensity, so that we expect that the source will be observable for the remainder of the useful life of Ariel-5.

Perhaps as important as the number of sources observed is a useful limit on the number which could have escaped detection. For sources more than 10° off the plane where source confusion is minimized, there were no sources which were as intense as 10% of the Crab Nebula for as much as a week (barring coincidence with the sun or the anti-spin axis, where there is no coverage by any Ariel-5 experiment). In the plane, where confusion can be problematic, the limit can range between 0.1 and ~ 0.5 of the Crab Nebula. The latter limit should, therefore, be a relatively firm upper limit for additional transient sources in the plane.

4. TRANSIENT SOURCE REMARKS

The most obvious conclusion which can be drawn from the Ariel-5 transient sources is that they appear to follow a galactic plane source distribution. This contrasts with the conclusion of Silk (1973) that the distribution is Population II (partly because of the ~ 20° galactic latitude of one of the four pre-Ariel-5 transients). It now appears certain that transients are largely confined to the galactic plane.

Assuming a right-cylindrical source volume, we can (after Silk) estimate the number of transients which exceed a limiting apparent magnitude S_o in a time t:

$$N(S_o,t) = \frac{t}{\tau}\,\frac{L}{4\pi S_o R^2}\,,$$

where τ is the mean time between source appearances with maximum luminosity L in the galaxy (of radius R). Solving for the only complete unknowns in terms of estimable quantities

$$\frac{L(\text{ergs s}^{-1})}{\tau(\text{yr})} = 3.6\times10^{38}\,\frac{N(>S_o,t)}{\tau(\text{yr})}\left(\frac{R(\text{kpc})}{15}\right)^2\left(\frac{S_o}{1.6\times10^{-8}}\right)$$

where 1.6×10^{-8} ergs $cm^{-2} sec^{-1}$ is the intensity of the Crab Nebula from the UHURU normalization. We cannot independently solve for L and τ, but can possible constrain one or the other by considering the upper limit to a galactic "ridge" which may be composed of contributions from transient sources of space density n_s:

$$L\,n_s < 8.6\times10^{-30}\ \text{ergs s}^{-1}\,\text{cm}^{-3}$$

from Holt, et al (1974). Since the source density must be approximately

$$n_s = \frac{1}{2\pi R^2 h}\,\frac{T}{\tau}$$

where h is the source disk half-thickness and T is the source "on-time" (i.e. the e-folding time for an exponentially decaying source). Solving for h,

$$h(\text{pc}) > 220\ N(>S_o,t)\,\frac{T(\text{mo})}{\tau(\text{yr})}\left(\frac{S_o}{1.6\times10^{-8}}\right)$$

it must be recalled that the expression only has meaning when the source on-time far exceeds the mean time between source appearances.

Considering that the transients appear to form at least two main classes, the soft-spectral long-decay sources yield (since $N = 3$ for $S = S_{crab}$ and $t = 1$)

$$\frac{L}{\tau} \approx 10^{39} \text{ ergs s}^{-1}\text{yr}^{-1}.$$

The failure of UHURU to detect more transient sources, as well as the failure of the All-Sky Monitor to detect any others > .3 Crab even though the ones at issue are so long-lasting, would indicate that τ can certainly be no smaller than 0.1 (i.e. no more than ten such sources per year at any apparent magnitude). This means that L is no smaller than ~ 10^{38} ergs s^{-1}, and such sources may well be Eddington-limited. This argument is self-consistent, in the sense that no sources of this type are expected at peak intensities below the All-Sky Monitor level of detectability. 10^{38} ergs s^{-1} sources, even at a distance of 25 kpc, will exhibit an intensity at maximum comparable to that of Crab Nebula.

With regard to the harder-spectral, shorter-duration sources, the situation is quite different. Here we obtain

$$\frac{L}{\tau} \sim 3\text{x}10^{38} \text{ ergs s}^{-1}\text{yr}^{-1},$$

where we are certainly battling detection threshold, and the shorter lifetime only makes the sources less easily detectable. It is worth noting, in this respect, that the only one of the four well-established pre-UHURU transients which is reconcilable with this subgroup (i.e. short lifetime), was the weakest of the four (2U1735-28) at a strength of about 0.5 Crab. We can argue, then, that we can make τ arbitrarily small to reduce the average maximum luminosity. The only restriction would appear to be from the lack of a ridge. As the sources last only $\sim$ two weeks, we would require $> 10^3 yr^{-1}$ ($\tau < 10^{-3}$) in order to sustain such a hypothetical ridge. But, as it would have a half-thickness 10^3 times too large to be reconcilable with a Population I source distribution, we must have $\tau > 10^{-3}$. I cannot think of any reason why it must be greater than $\tau \sim 10^{-2}$, which would give these sources rather modest luminosities $< 10^{37}$ erg sec. This might be reasonable in view of the similarity of these sources with Vel X-1. The latter system is driven by the stellar wind of a supergiant, which typically gives rise to sub-Eddington luminosities. There is no reason why there cannot be $\sim$ 100 of these sources per year in the galaxy.

5. SCO X-1   Sco X-1 is the only source which allows any detailed analysis of the orbit-by-orbit measurements. Typically, we obtain $\sim$ 300 counts per element per orbit from Sco X-1, compared to $\sim$ 20 from the Crab Nebula, the next strongest source. Figure 5 illustrates the obvious lack of source constancy from one orbit to the next. Nevertheless, the long baseline enables us to average over these variations when we test for a known trial period. Figure 6 illustrates the result of folding $\sim$ 200d worth of data modulo .787313d, the candidate optical period of Sco X-1 (Gottlieb, Wright and Liller, 1975). The lack of observable modulation places an upper limit on the x-ray modulation amplitude of $\sim$ 1%, more than an order of magnitude below the optical modulation amplitude.

Sco X-1 is not completely chaotic, however. Figure 7, from a particularly disturbed period, illustrates that the large intensity variations appear to correlate on time scales larger than one orbit. We have attempted to treat the problem as a classical shot noise disturbance, as we did on shorter time scales for Cyg X-1 (c.f. Boldt, Holt, Rothschild and Serlemitsos, 1975). At first glance, Figure 8 would appear to be a great disappointment for the model, as the characteristic flattening is not exhibited for times greater than the shot noise duration. We have found, however, that there is, in fact, a persistent correlation time of 4-5 orbits (~ 1/3 d) for a large fraction (perhaps half) of the Sco X-1 counting rate. It is important to note that such correlation does not imply that half the Sco X-1 counting rate waxes and wanes with a time scale of 1/3 day but that roughly this fraction is composed of pulses which individually last that long. At any time, there are tens of such individual pulses "on". A complete description of this analysis is presently in progress (Holt, Boldt, Serlemitsos and Kaluzienski, 1975a).

6. CYG X-3 The long-term monitoring of sources below the level of Sco X-1 is also possible with the All-Sky Monitor, albeit with much lower sensitivity. We can observe regular behavior of other sources even from single-orbit data, as evidenced by Figure 9. Here Cyg X-3 data from ~ 100 days has been folded modulo the 4.8h period previously determined from other investigations, and both the shape and phase of the modulation are entirely consistent with previous reports (c.f. Leach, et al. 1975).

Figure 10 illustrates the long-term behavior of Cyg X-3 in daily averages, which are indicative of a widely varying source intensity. Although there are many trial period which give relative χ^2 maxima, there is a systematic indication of a 17d effect. Figure 11 combines all the data in Figure 10 folded at 17d, and the χ^2 distribution yields 17.0 $\pm$.3d with a phase at maximum of JD 2,440, 2387$\pm$2 near the most pronounced peak. Evidence from the Ariel-5 Sky Survey Experiment (Pounds, private communication, 1975) is consistent with the reported effect, in the sense that the three maxima observed by the Sky Survey Experiment (in the gaps of Figure 10) are consistent with both the All-Sky Monitor period and phase. This 17d variation may represent a quasi-periodic variation similar to the 35d variation in Her X-1, or a more fundamental period. If it is the system binary period, the 4.8h variation would have to be reinterpreted in terms of source rotation, which would make Cyg X-3 even more anomalous an X-ray source than it presently is believed to be.

7. CYG X-1 We have positively detected a 5.6d modulation of the Cyg X-1 intensity, which virtually clinches the identification of that source with HDE 226868. Figure 12 is a long-term display of the daily average intensity of Cyg X-1, which clearly indicates the relative lack of a day-to-day variation in the source intensity until the flare of April-May 1975. The rise to maximum of the flare was observed by the All-Sky Monitor until the spin axis was pointed to Cyg X-1, and the daily and $\sim \frac{1}{2}$ day data are shown in Figures 13 and 14 (from Holt, et. al. 1975b). The few-day variation in the source intensity is characteristic of both the rise and the fall of the increase (c.f. Sanford et. al. 1975), so that models for the instability should reflect a factor-of-two variation on a timescale of a few days.

All of the data in Figure 12 (excluding the April-May increase) have been folded at trial periods in the neighborhood of 5.6d, with the distribution of the resultant χ^2 exhibited in Figure 15. A significant modulation is found at 5.605$\pm$.008d from this distribution alone, which includes the HDE 226868 period of 5.60089 (from the Copernicus ephemeris). The five-bin light curve is displayed in Figure 16, which clearly defines the predominant feature of the variation to be a minimum near superior conjunction. As described in more detail in Holt, et al. (1975c), the fractional light curve decrement at superior conjunction of .027 $\pm$.004 found in these data is an order of magnitude more pronounced than one would expect from the published observations of "absorption dips".

A possible clue to the nature of the effect is given by Figure 17, wherein it can be observed that the depth of modulation as well as the average source intensity apparently increase with time until the April-May flare. The modulation may represent a shadowing of the hard x-ray emitting region by material which then serves a fuel for the gradually increasing intensity, until a system instability which is manifested in the flare readjusts the source to its pre-buildup level.

8. SUMMARY The present results are meant to demonstrate the studies presently undertaken with data from the All-Sky Monitor. The first year of operation has been highly successful for all the experiments aboard Ariel-5, and the next year is eagerly anticipated. With respect to the All-Sky Monitor alone, the doubling of the data base should enable the discovery of another half-dozen transient sources, as well as the continuation of long-term source investigations similar to those reported here.

Figure Captions:

1. The light curve of A1524-62. The points are data from the All-Sky Monitor accumulated over 3-7 orbits, while the solid trace is a representation of the Sky Survey Experiment data normalized to the natural All-Sky Monitor ordinate.
2. The decay of A0536+26 from All-Sky Monitor 3-7 orbit accumulations.
3. The rise and fall of the flare in Aql X-1 in 3-7 orbit All-Sky Monitor accumulations.
4. The early decay of A0620-00. The All-Sky Monitor data points are daily averages (half-days near maximum), with typical error bars < 2%. The dashed trace is obtained from IAU circulars with reports from other Ariel-5 instruments, normalized to the Crab Nebula. The obvious difference at peak is attributed to the soft A0620-00 spectrum relative to that of the Crab.
5. Single-orbit intensity measurements of Sco X-1. The statistical errors are $\pm$ 1σ.
6. > 200 days of Sco X-1 data folded modulo .787313d. The "expected minimum" is the phase of the optical minimum.
7. Orbit-by-orbit Sco X-1 data for a time interval during which the intensity was changing more frequently (and with larger amplitude) than usual. Note, particularly, the multiple-orbit duration of the variations.
8. The "variance ratio" $<\frac{(x_i-\bar{x})^2}{\delta^2 x_i}>$ for $\sim 10^3$ orbits of Sco X-1 data. δx_i is the statistical error in the source intensity x_i. λ is the candidate shot-noise rate (orbit^{-1}) and τ the shot duration (in orbits).

PRECEDING PAGE BLANK NOT FILMED

9. Single-orbit Cyg X-3 data folded modulo 4.8h.
10. Daily average intensities for Cyg X-3. The squares above the figure are the positions of the 17d maxima expected from Figure 11.
11. Results of folding the Cyg X-3 data at periods near 17d. The χ^2 distribution yields 17.0 $\pm$0.3d as the candidate period. The 17.0d folds for Cyg X-3 are at two phases displaced by 1/2-bin, with Cyg X-1 used as a control.
12. Daily average intensities for Cyg X-1.
13. Daily average Cyg X-1 intensities at the time of the April 1975 increase.
14. The same data as in Figure 13 with ~ 1/2-day resolution.
15. Results of folding the Cyg X-1 data at periods near 5.6d. The χ^2 distribution yields 5.605 $\pm$.008d as the candidate period.
16. Cyg X-1 and Crab Nebula data folded modulo 5.60089d.
17. The data of Figure 12 broken into 56-day periods for which individual 5.6d folds and average intensities are displayed.

References

Boldt, E. A., Holt, S. S., Rothschild, R. E. and Serlemitsos, P. J. 1975, Proc. Intl. Conf. X-Rays in Space, Univ. of Calgary

Elvis, M., Griffiths, R. G., Turner, M. J. L. and Page, C. G. 1975 IAU Circular No. 2814

Eyles, C. J. et al. 1975 IAU Circular No. 2774

Gottlieb, E. W., Wright, E. L. and Liller, W. 1975 Astrophys. J. Letts. 195, L33

Holt, S. S. 1975 Proc. COSPAR Symp. Fast Transients X- and Gamma-Ray Astron., Astrophys. Space Sci., in the press

Holt, S. S., Boldt, E. A., Serlemitsos, P. J. and Kaluzienski, L. J. 1975a, in preparation

Holt, S. S., Boldt, E. A., Serlemitsos, P. J. and Kaluzienski, L. J. 1975c Astrophys. J. Letts., in the press.

Holt, S. S., Boldt, E. A., Kaluzienski, L. J. and Serlemitsos, P. J. 1975b Nature 256, 108

Holt, S. S., Boldt, E. A., Serlemitsos, P. J., Murray, S. S., Giacconi, R., Kellogg, E. M. and Matilsky, T. A. 1974 Astrophys. J. Letts. 188, L97

Ives, J., Sanford, P. W. and Bell Burnell, S. J. 1975 Nature 245, 578

Kaluzienski, L. J., Holt, S. S., Bold , E. A. and Serlemitsos, P. J. 1975 Nature 256, 633

Kaluzienski, L. J., Holt, S. S., Boldt, E. A., Serlemitsos, P. J., Eadie, G., Pounds, K. A., Ricketts, M. J. and Watson, M. 1975 Astrophys. J. Letts., in the press

Leach, R. W., Murray, S. S., Schreier, E. J., Tananbaum, H. D. and Ulmer, M. P. 1975, Astrophys. J. 199, 184

Pounds, K. A. 1974 IAU Circular No. 2729

Sanford, P. W., Ives, J. C., Bell Burnell, S. J., Mason, K. O. and Murdin, P. 1975 Nature 256, 109

Silk, J. 1973 Astrophys. J. 181, 747

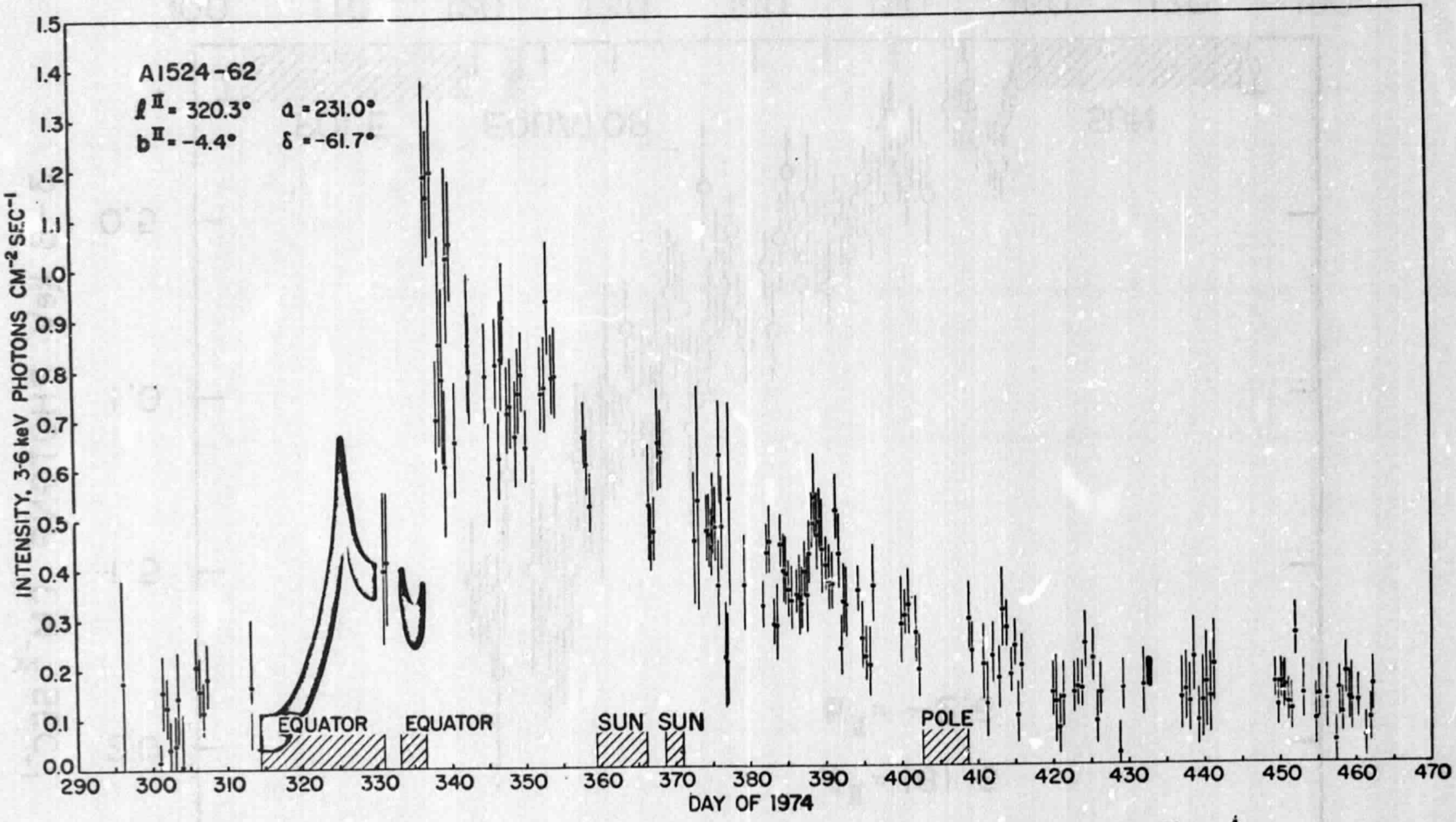
A1524-62
ℓ^{II} = 320.3°
α = 231.0°
b^{II} = -4.4°
δ = -61.7°
INTENSITY, 3-6 keV PHOTONS CM^{-2} SEC^{-1}
DAY OF 1974
EQUATOR
EQUATOR
SUN
SUN
POLE

Fig. 1

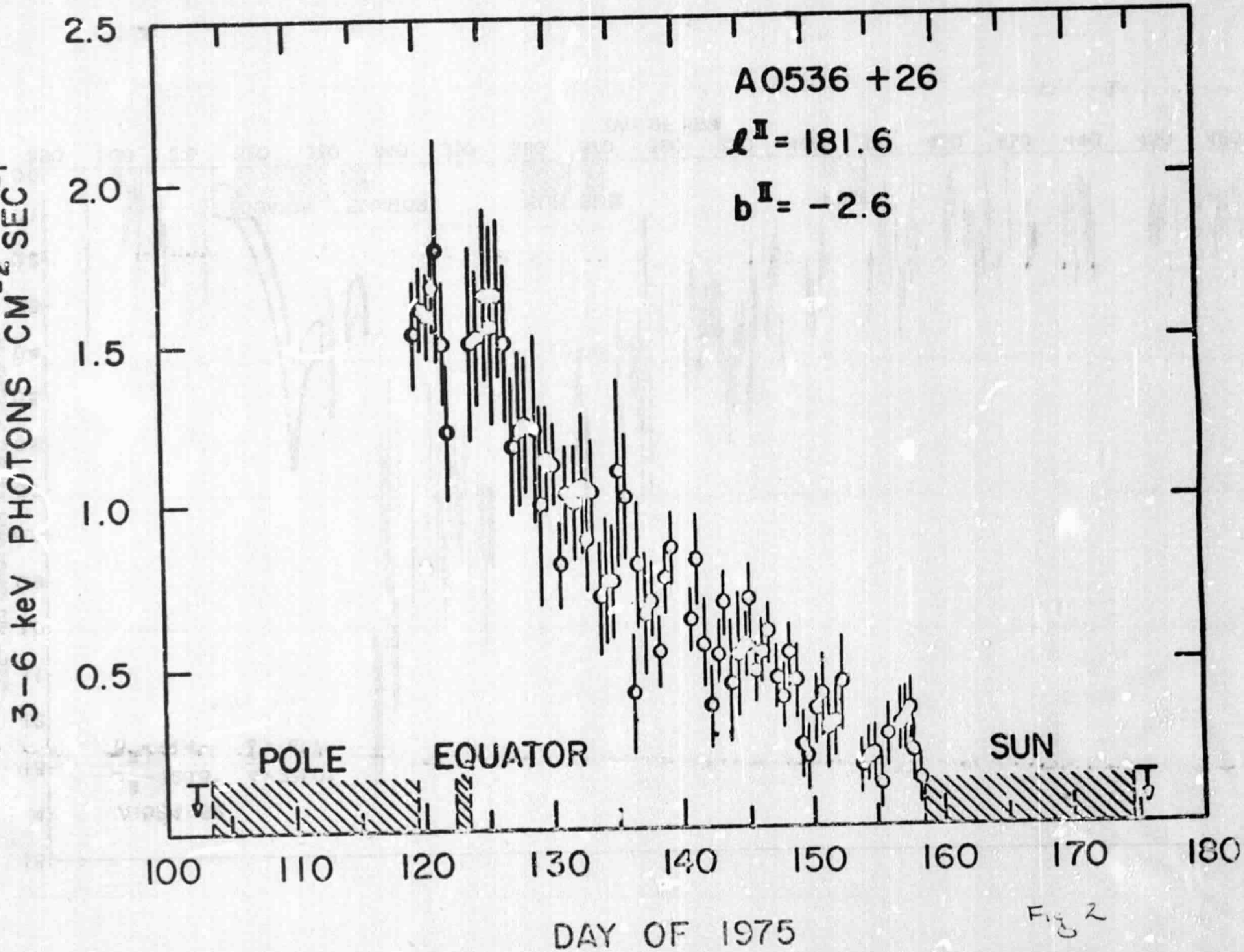
A0536 +26
ℓ^{II} = 181.6
b^{II} = -2.6
3-6 keV PHOTONS CM^{-2} SEC^{-1}
2.5
2.0
1.5
1.0
0.5
POLE
EQUATOR
SUN
100
110
120
130
140
150
160
170
180
DAY OF 1975

Fig 2

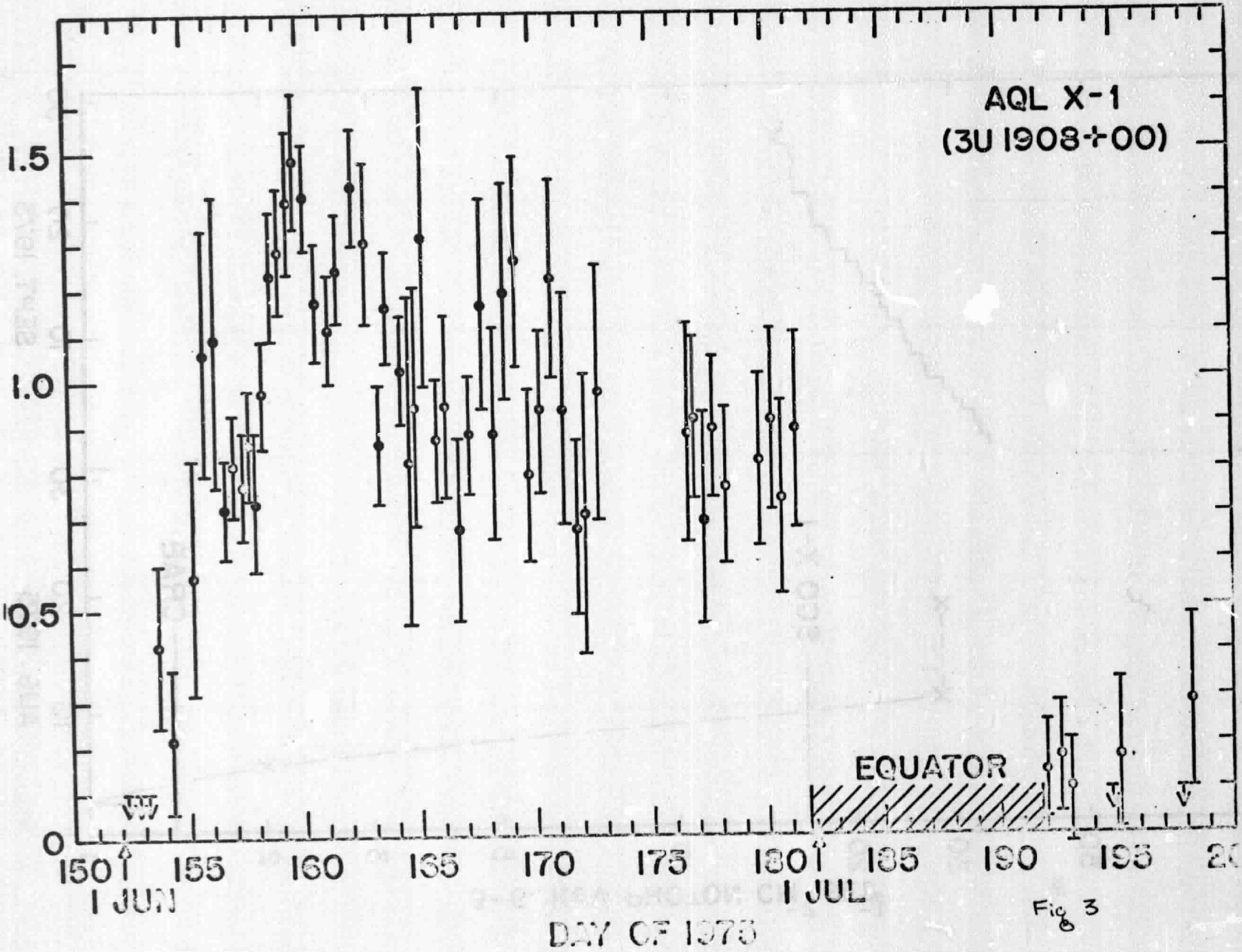
AQL X-1
(3U 1908+00)
EQUATOR
1.5
1.0
0.5
0
150
155
160
165
170
175
180
185
190
195
1 JUN
1 JUL
DAY OF 1975

Fig 3

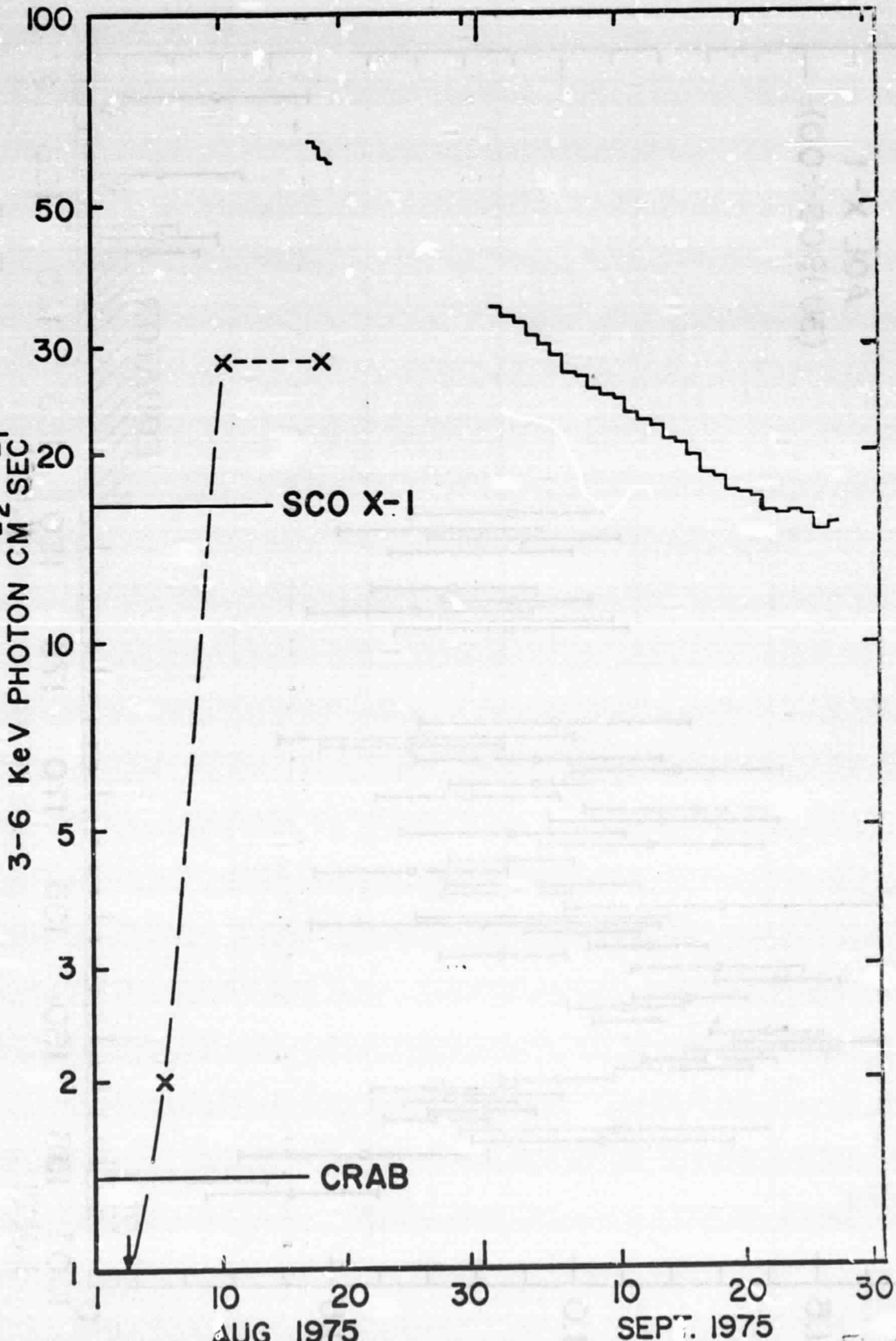

100
50
30
20
10
5
3
2
1
3-6 KeV PHOTON CM^{-2} SEC^{-1}
SCO X-1
CRAB
1
10
20
30
10
20
30
AUG 1975
SEPT. 1975

Fig. 4

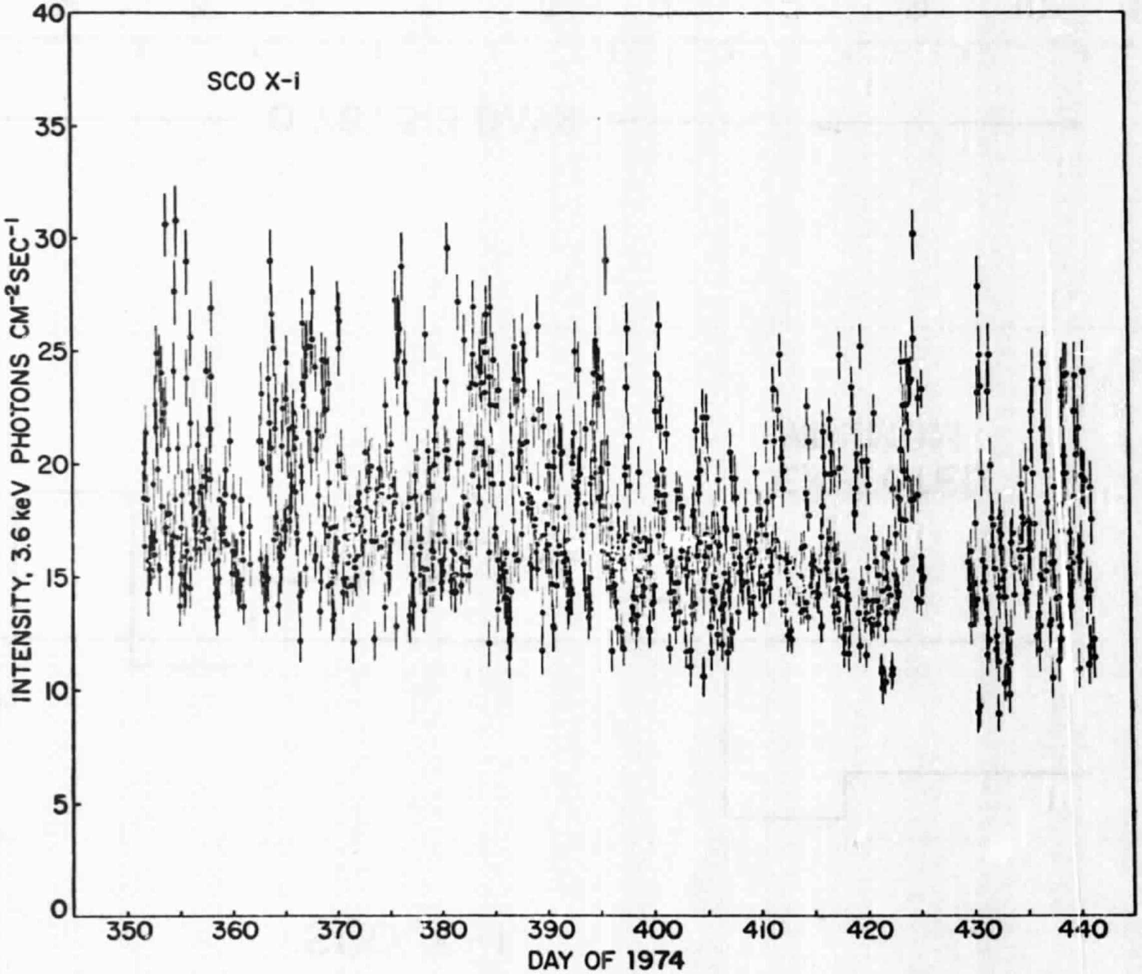
SCO X-1
INTENSITY, 3.6 keV PHOTONS CM^-2 SEC^-1
0
5
10
15
20
25
30
35
40
350
360
370
380
390
400
410
420
430
440
DAY OF 1974

Fig 5

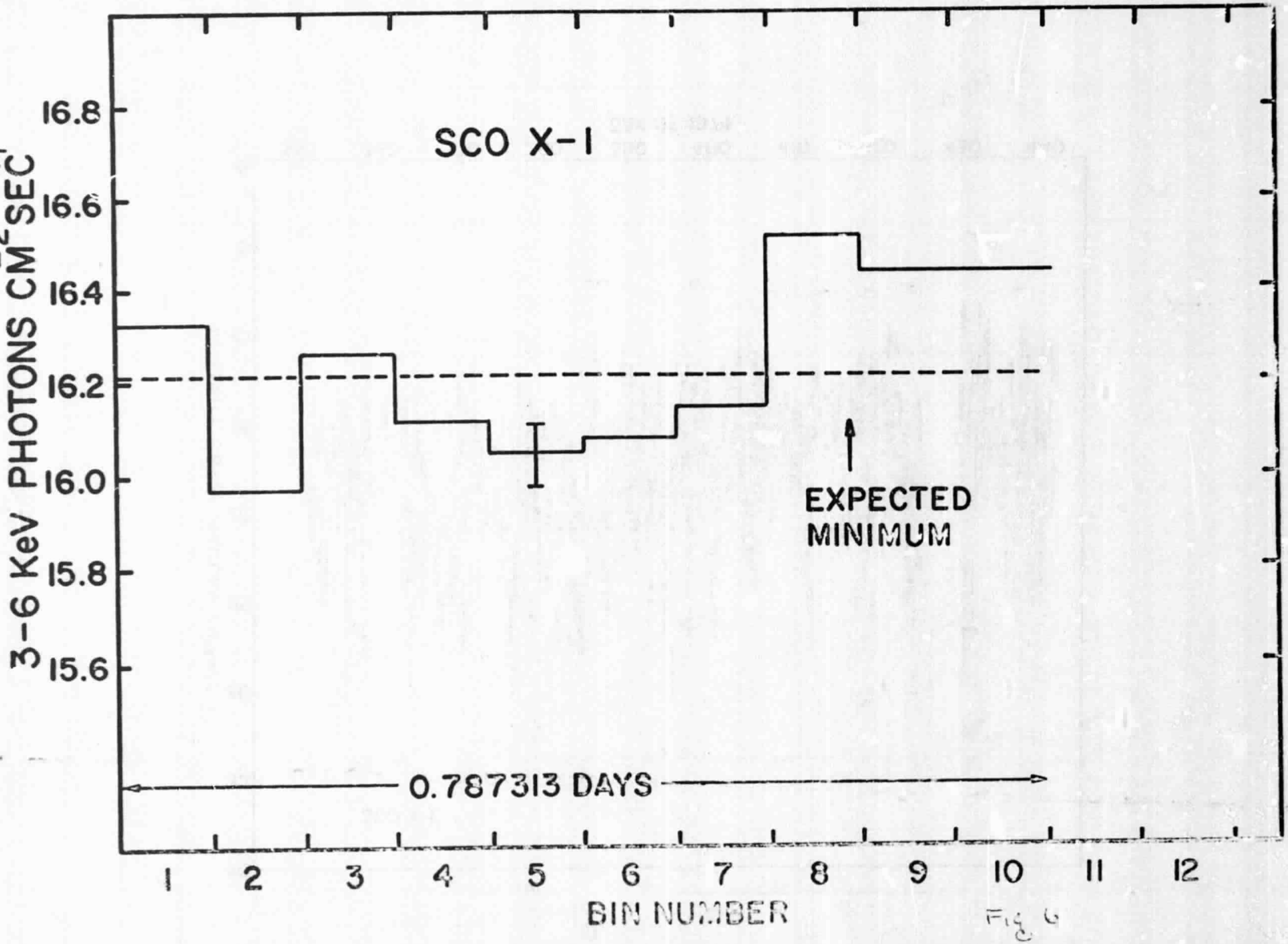
SCO X-1
3-6 KeV PHOTONS CM^{-2}SEC^{-1}
16.8
16.6
16.4
16.2
16.0
15.8
15.6
EXPECTED MINIMUM
0.787313 DAYS
1
2
3
4
5
6
7
8
9
10
11
12
BIN NUMBER

Fig. 6

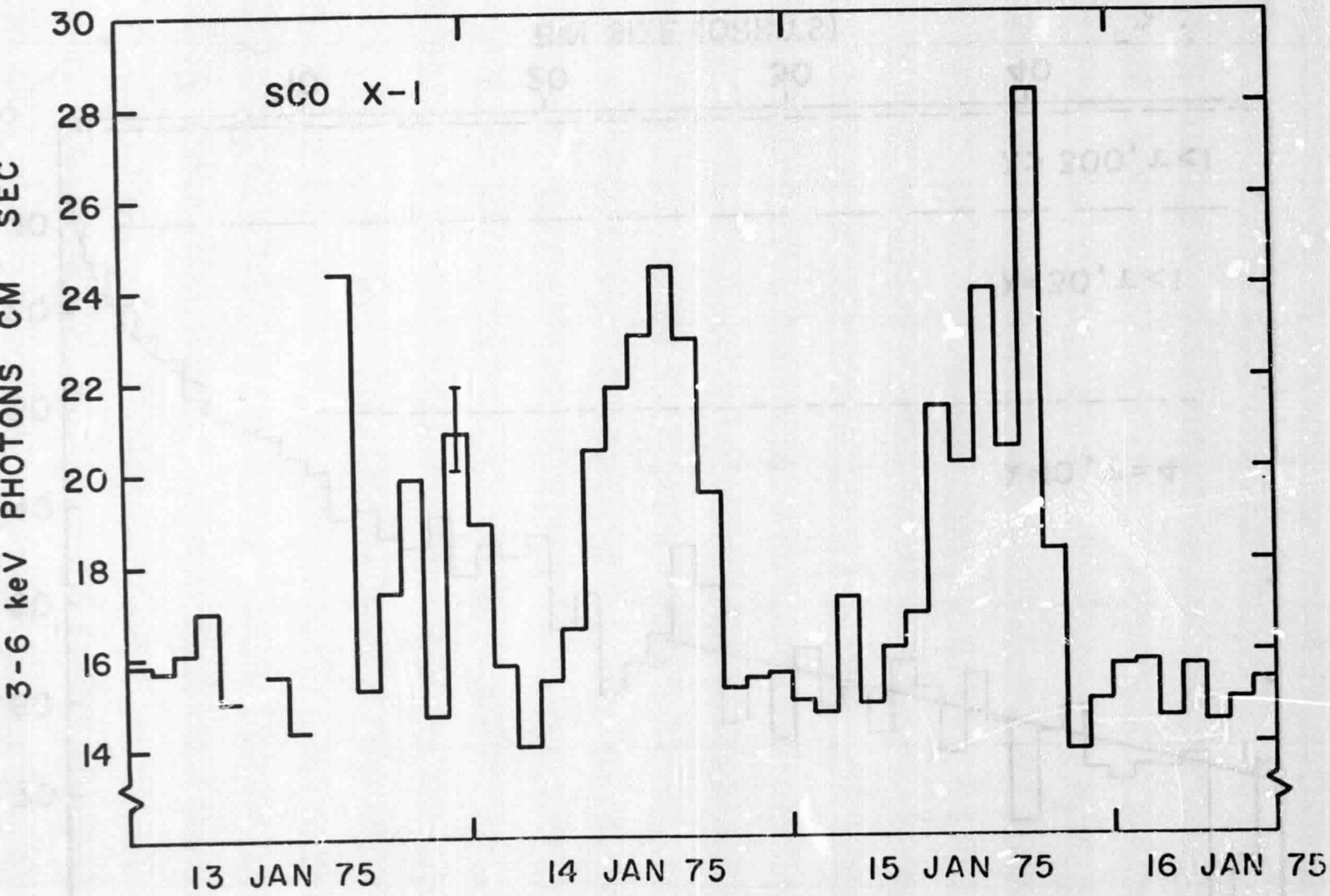
SCO X-1
3-6 keV PHOTONS CM^{-2} SEC^{-1}
30
28
26
24
22
20
18
16
14
13 JAN 75
14 JAN 75
15 JAN 75
16 JAN 75

Fig 7

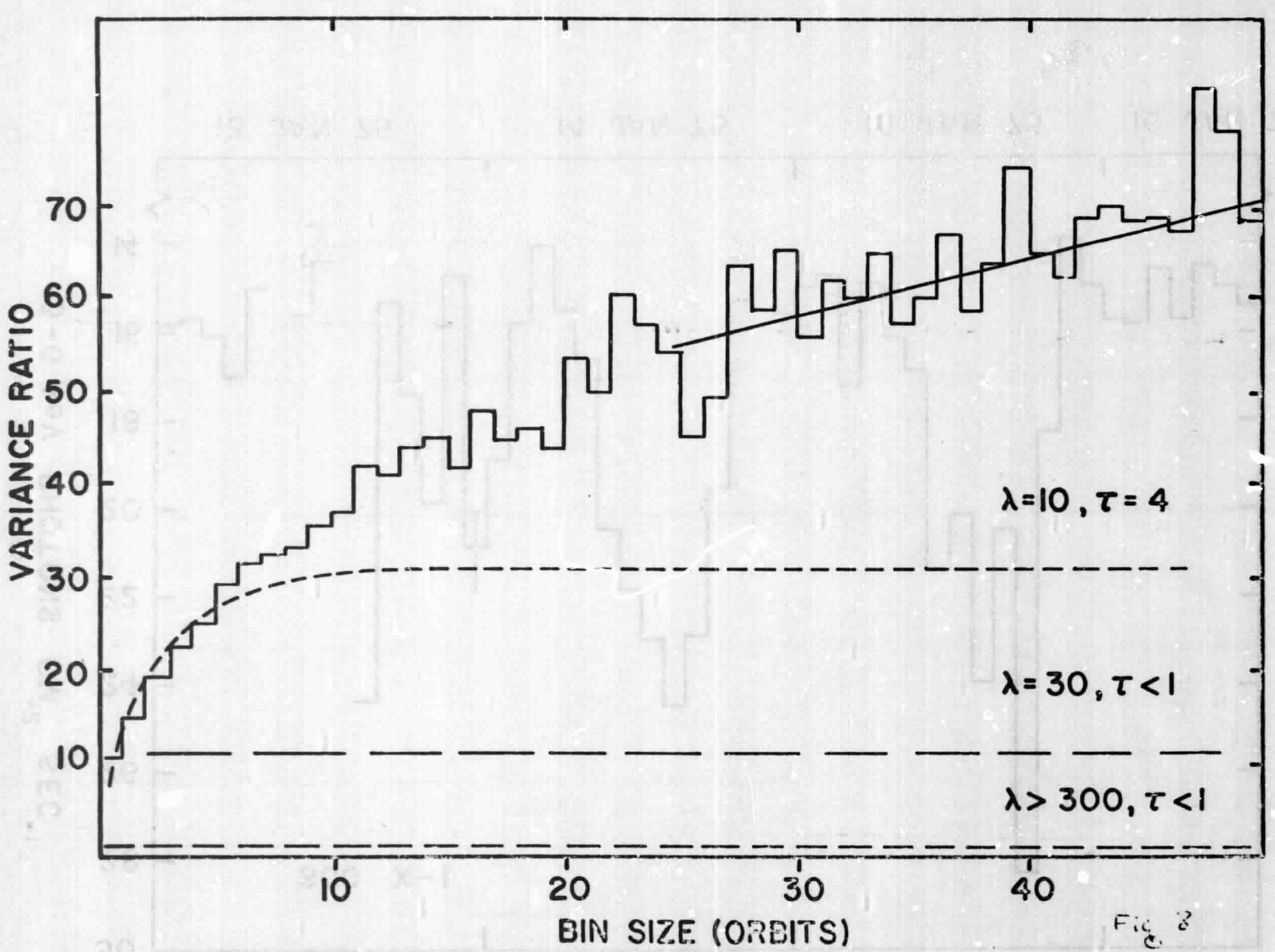

70
60
50
40
30
20
10
VARIANCE RATIO
10
20
30
40
BIN SIZE (ORBITS)
λ=10 , τ = 4
λ= 30, τ <1
λ> 300, τ <1

Fig. 8

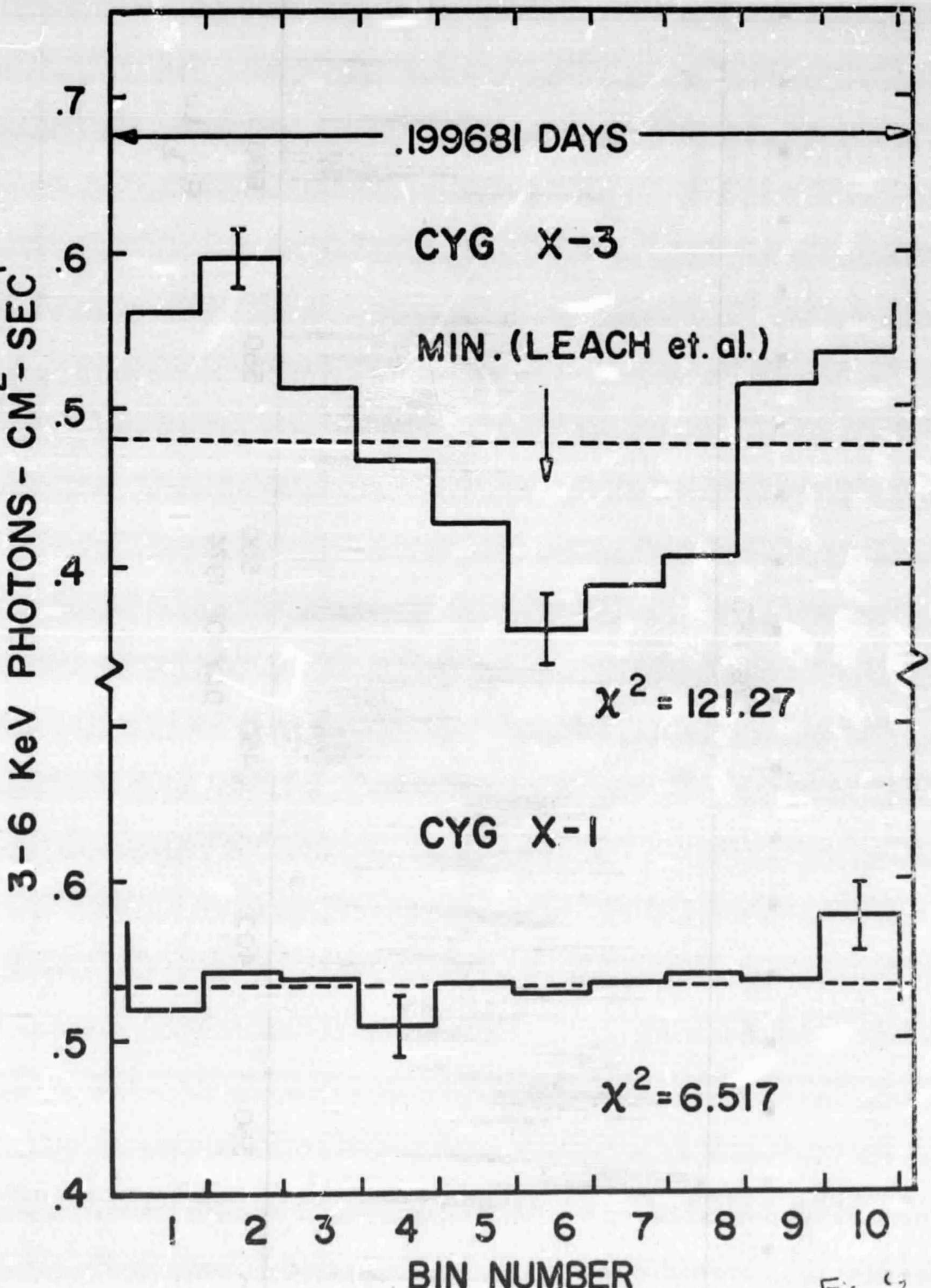

.199681 DAYS
CYG X-3
MIN. (LEACH et. al.)
$X^2 = 121.27$
CYG X-1
$X^2 = 6.517$
3-6 KeV PHOTONS - CM^{-2} - SEC^{-1}
.7
.6
.5
.4
.6
.5
.4
1
2
3
4
5
6
7
8
9
10
BIN NUMBER

Fig 3

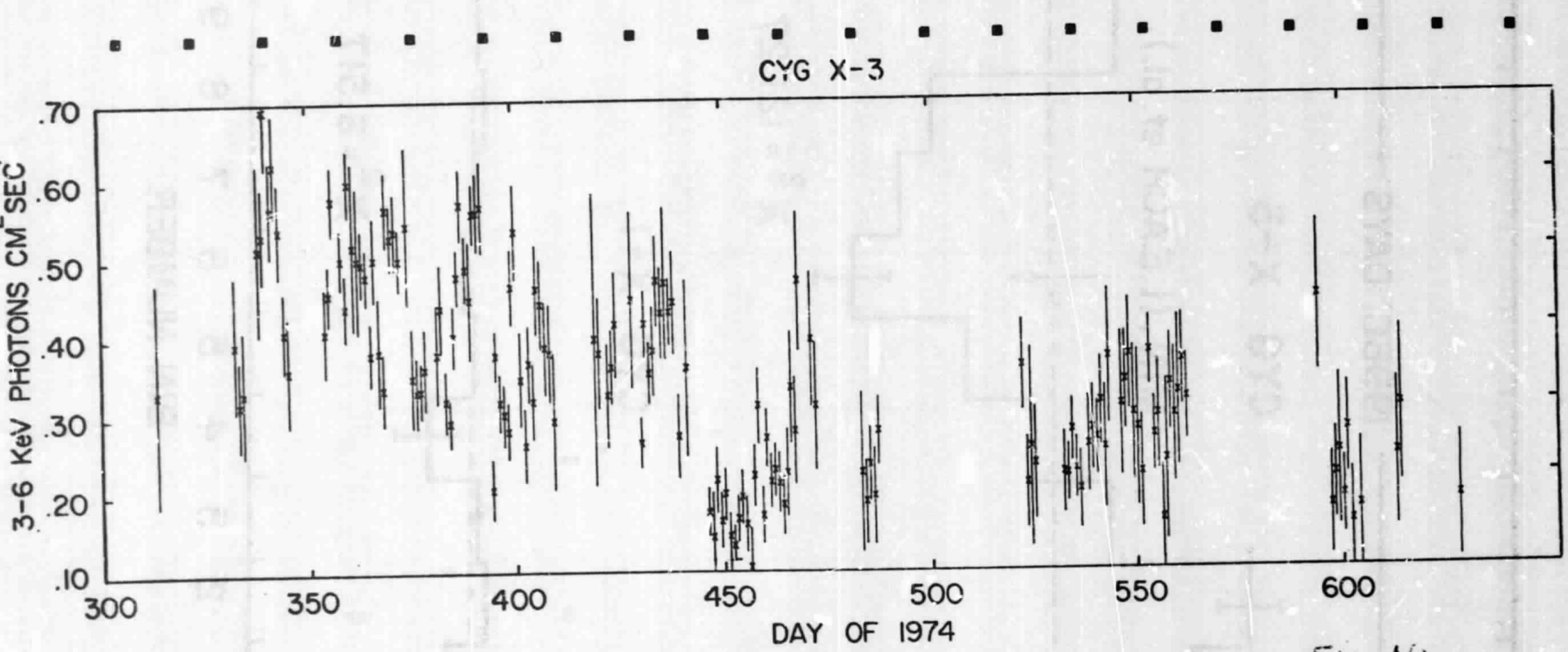
CYG X-3
3-6 KeV PHOTONS CM^{-2}SEC^{-1}
.70
.60
.50
.40
.30
.20
.10
300
350
400
450
500
550
600
DAY OF 1974

Fig. 10

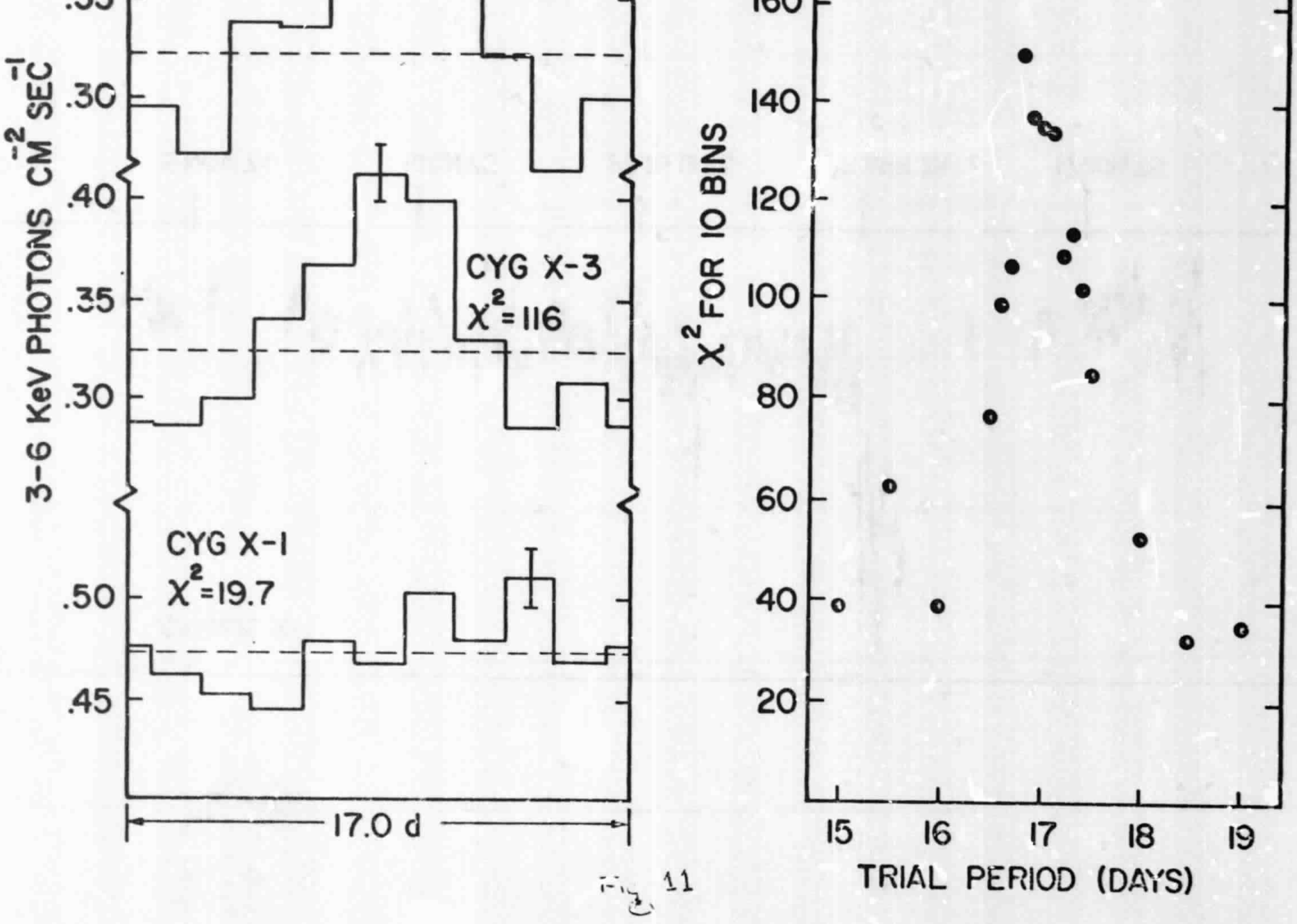
3-6 KeV PHOTONS CM^{-2} SEC^{-1}
CYG X-3
X^2=135
CYG X-3
X^2=116
CYG X-1
X^2=19.7
17.0 d
X^2 FOR 10 BINS
TRIAL PERIOD (DAYS)

Fig. 11

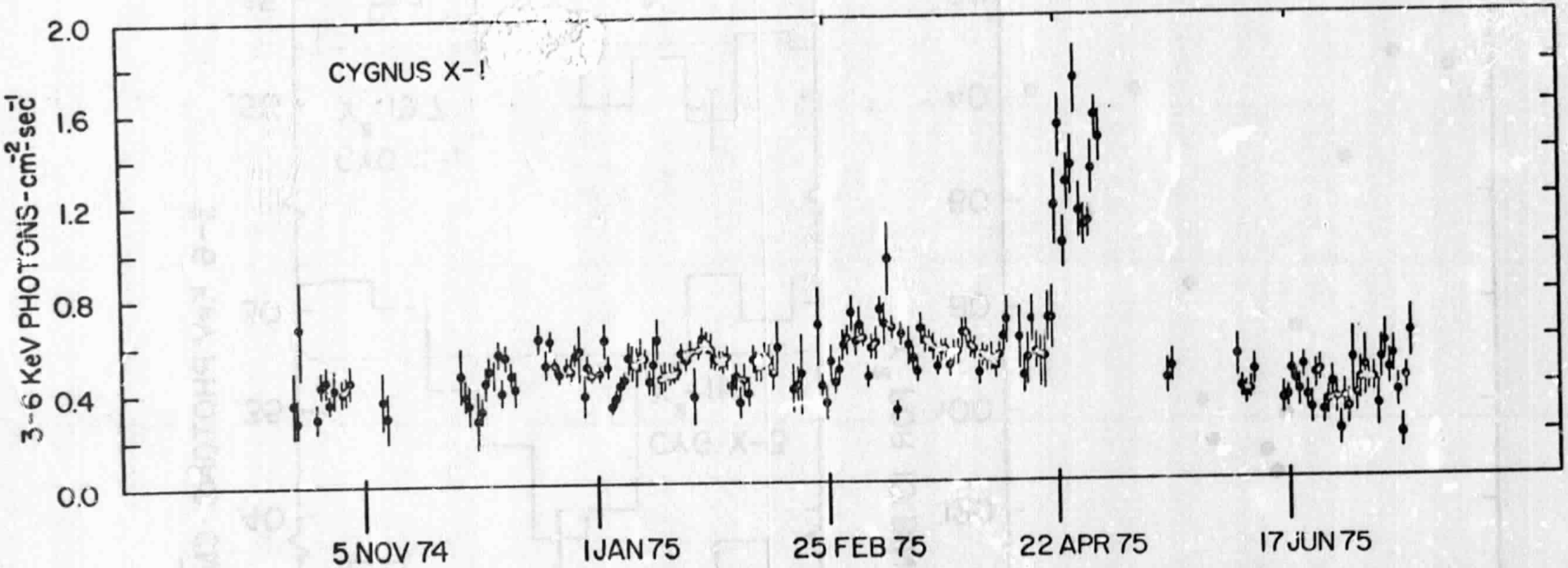
CYGNUS X-1
3-6 KeV PHOTONS-cm-2-sec-1
2.0
1.6
1.2
0.8
0.4
0.0
5 NOV 74
1 JAN 75
25 FEB 75
22 APR 75
17 JUN 75

Fig. 12

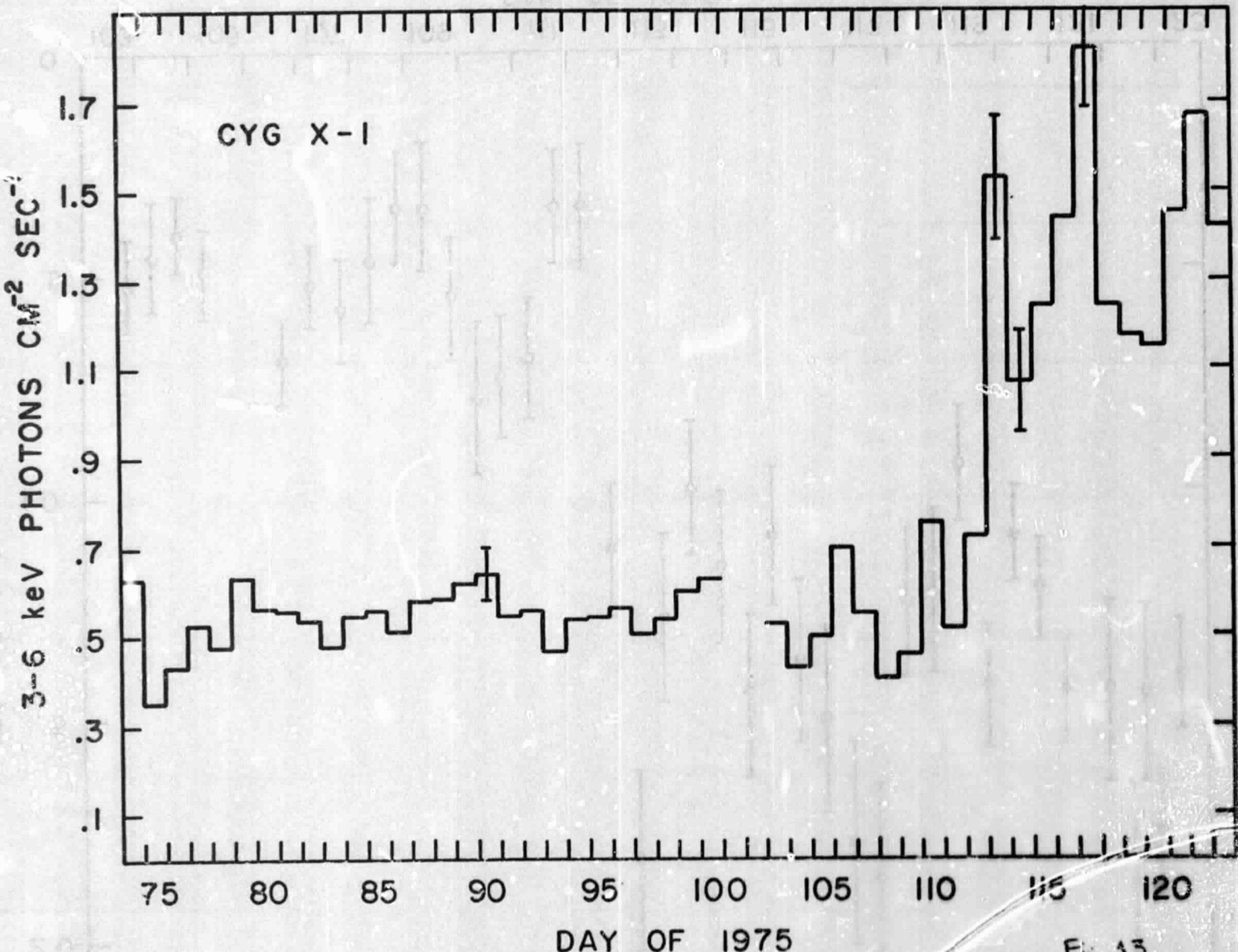
CYG X-1
3-6 keV PHOTONS CM^{-2} SEC^{-1}
1.7
1.5
1.3
1.1
.9
.7
.5
.3
.1
75
80
85
90
95
100
105
110
115
120
DAY OF 1975

Fig. 13

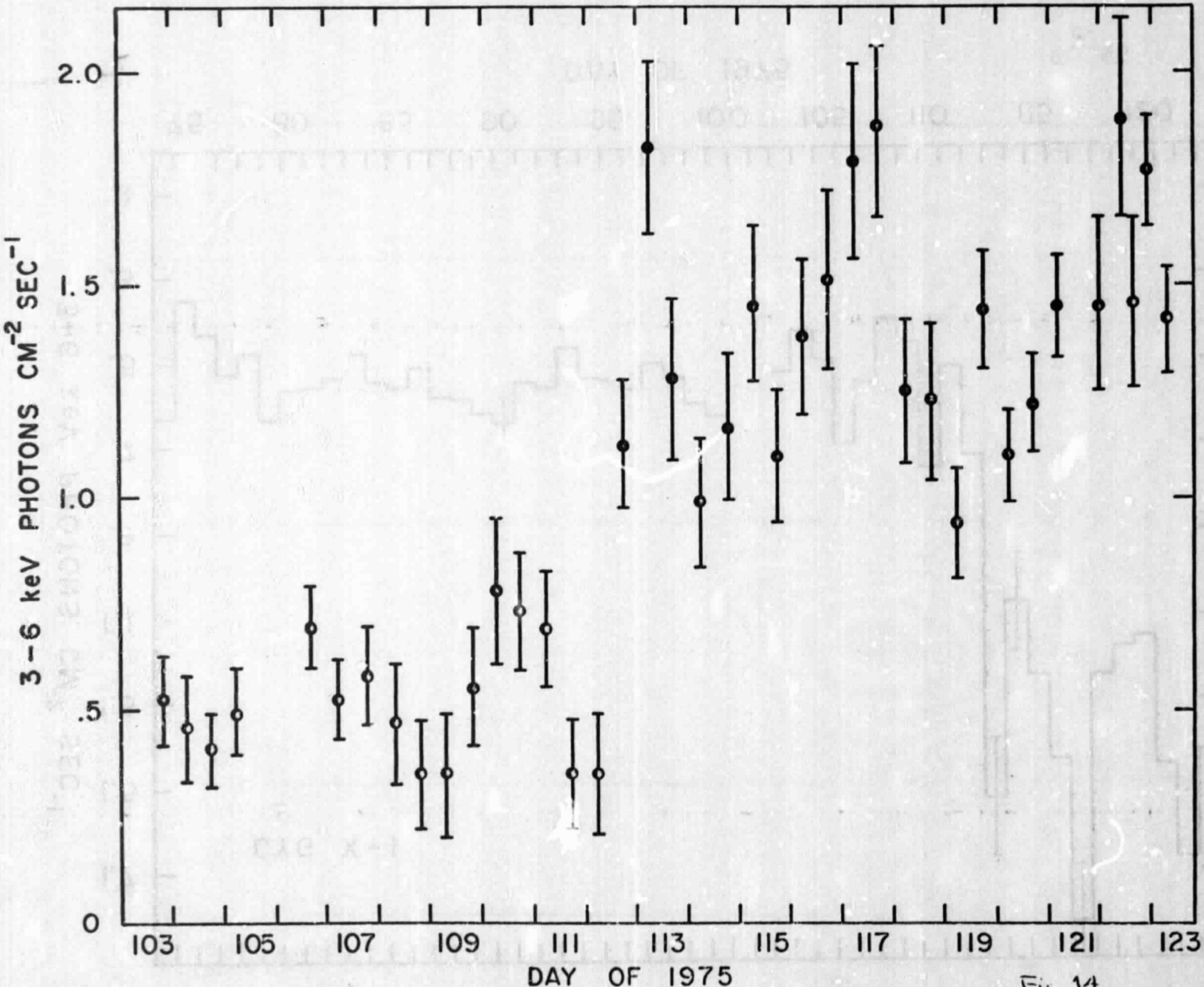
3-6 keV PHOTONS CM^{-2} SEC^{-1}
2.0
1.5
1.0
.5
0
103
105
107
109
111
113
115
117
119
121
123
DAY OF 1975

Fig 14

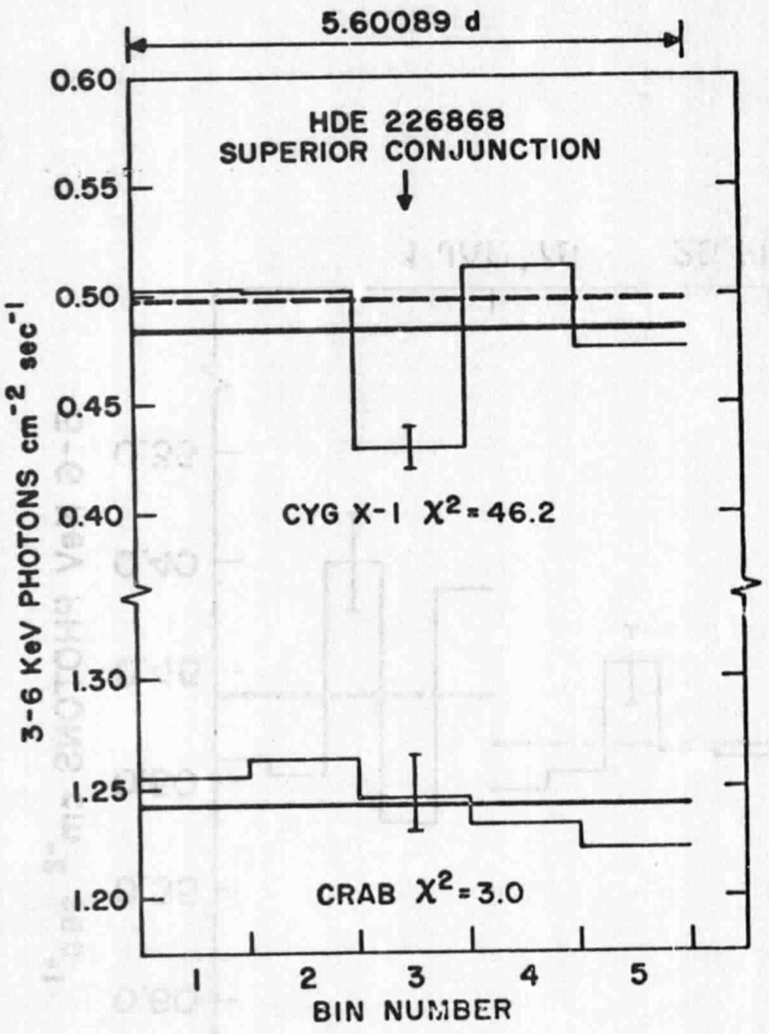
5.60089 d
HDE 226868
SUPERIOR CONJUNCTION
0.60
0.55
0.50
0.45
0.40
1.30
1.25
1.20
3-6 KeV PHOTONS cm^{-2} sec^{-1}
CYG X-1 X^2 = 46.2
CRAB X^2 = 3.0
1
2
3
4
5
BIN NUMBER

Fig. 16

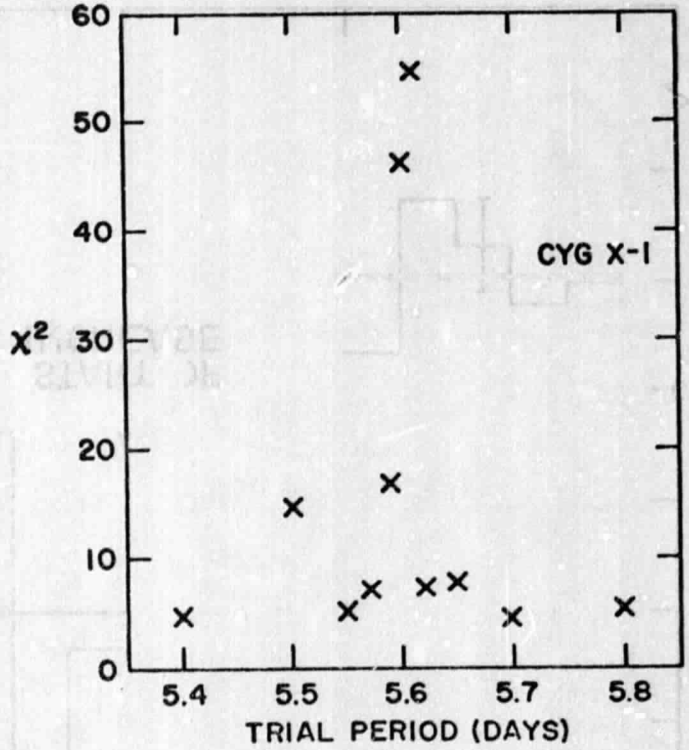
60
50
40
30
20
10
0
X^2
CYG X-1
5.4
5.5
5.6
5.7
5.8
TRIAL PERIOD (DAYS)

Fig. 15

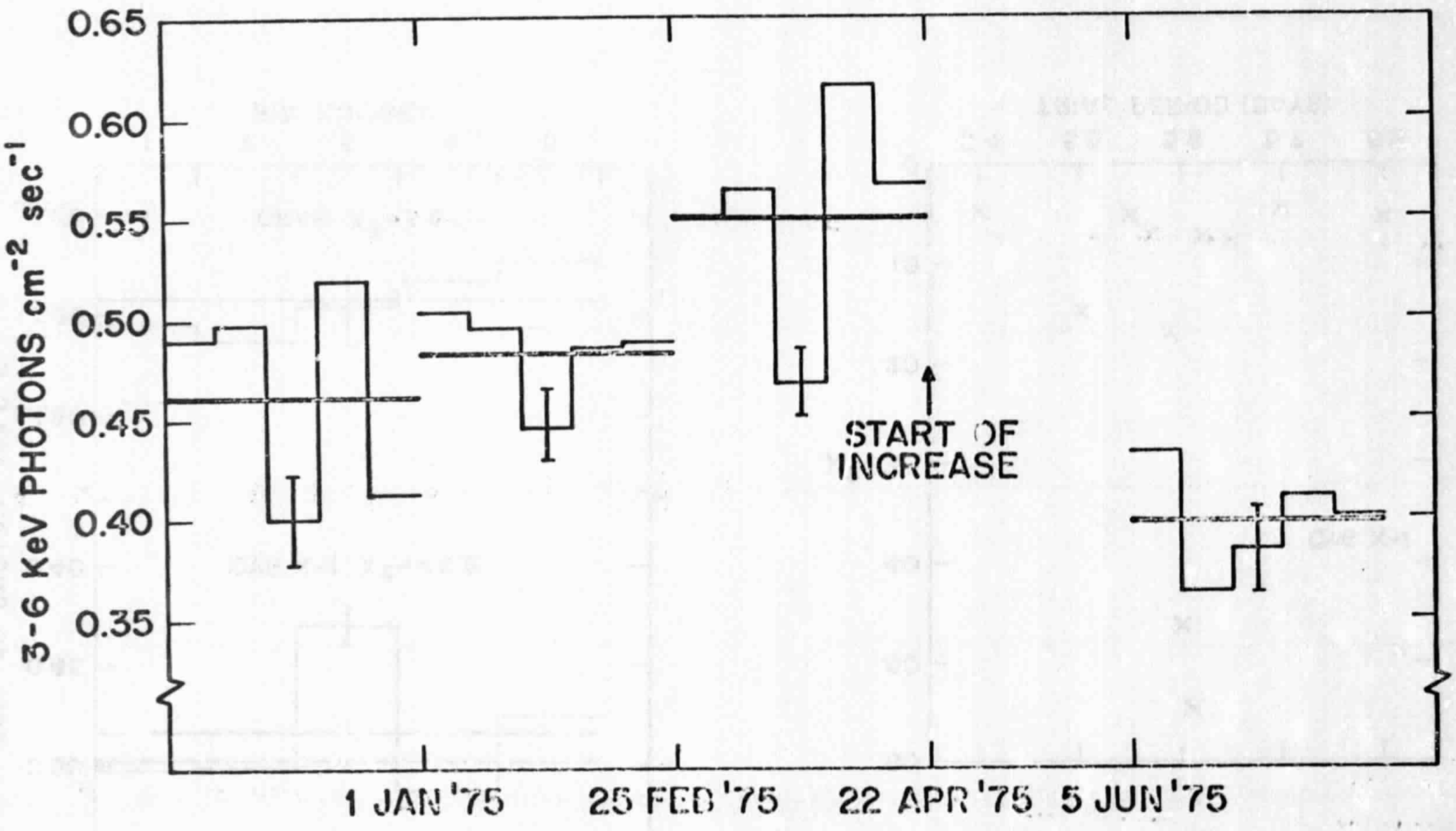
0.65
0.60
0.55
0.50
0.45
0.40
0.35
3-6 KeV PHOTONS cm-2 sec-1
START OF
INCREASE
1 JAN '75
25 FEB '75
22 APR '75
5 JUN '75

Fig. 17